Urologia Internationalis

Research Article

Urol Int 2024;108:49–59
DOI: 10.1159/000535025

Received: May 28, 2023
Accepted: October 14, 2023
Published online: November 30, 2023

Metformin Regulates the miR-205/VEGFA Axis in Renal Cell Carcinoma Cells: Exploring a Clinical Synergism with Tyrosine Kinase Inhibitors

Markus Krebs[a, b] Mischa J. Kotlyar[a, c] Julian Fahl[a] Sudha Janaki Raman[d] Florian Röhrig[d] André Marquardt[b, e] Hubert Kübler[a] Burkhard Kneitz[a] Almut Schulze[d, f] Charis Kalogirou[a]

[a]Department of Urology and Pediatric Urology, University Hospital Würzburg, Würzburg, Germany; [b]Comprehensive Cancer Center Mainfranken, University Hospital Würzburg, Würzburg, Germany; [c]Department of Interdisciplinary Critical Care Medicine and Intermediate Care, Helios Clinic Erfurt, Erfurt, Germany; [d]Chair of Biochemistry and Molecular Biology, Biocenter, University of Würzburg, Würzburg, Germany; [e]Institute of Pathology, Klinikum Stuttgart, Stuttgart, Germany; [f]Division of Tumor Metabolism and Microenvironment, German Cancer Research Center, Heidelberg, Germany

Keywords
Metformin · MicroRNA · Tyrosine kinase inhibitor · Kidney cancer · Angiogenesis

Abstract
Introduction: Metformin (MF) intake could be associated with a favorable outcome in sunitinib (SUT)- and axitinib (AX)-treated clear cell renal cell carcinoma (ccRCC) patients. Functionally, MF induces miR-205, a microRNA serving as a tumor suppressor in several cancers. ***Methods:*** Real-time quantitative PCR, viability assays, and Western blotting analyzed MF and SUT/AX effects in RCC4 and 786-O cells. A tetracycline-inducible overexpression model was used to study the role of miR-205 and its known target gene, *VEGFA*. We analyzed miR-205 and *VEGFA* within a public and an in-house ccRCC cohort. Human umbilical vein endothelial cell (HUVEC) sprouting assays examined miR-205 effects on angiogenesis initiation. To determine the influence of the von Hippel-Lindau tumor suppressor (*VHL*), we examined *VHL*^{wt} reexpressing RCC4 and 786-O cells. ***Results:*** Viability assays confirmed a sensitizing effect of MF toward SUT/AX in RCC4 and 786-O cells. Overexpression of miR-205 diminished *VEGFA* expression – as did treatment with MF. Tumor tissue displayed a downregulation of miR-205 and an upregulation of *VEGFA*. Accordingly, miR-205 caused less and shorter vessel sprouts in HUVEC assays. Finally, *VHL*^{wt}-expressing RCC4 and 786-O cells displayed higher miR-205 and lower *VEGFA* levels. ***Conclusion:*** Our results support the protective role of MF in ccRCC and offer functional insights into the clinical synergism with tyrosine kinase inhibitors.

Introduction

Preclinical and epidemiological studies in several malignancies suggest a tumor-suppressive role of metformin (MF), a biguanide originally used for treating type 2 diabetes [1]. There is increasing evidence that combining MF and antineoplastic agents may improve outcomes of patients suffering from lung [2], colorectal, and prostate cancer [3]. Regarding clear cell renal cell

karger@karger.com
www.karger.com/uin

Correspondence to:
Charis Kalogirou, kalogirou_c@ukw.de

carcinoma (ccRCC), regular MF intake was associated with a lower cancer incidence in patients with type 2 diabetes [4]. Moreover, two recent studies identified regular MF intake as prognostically favorable in ccRCC patients treated with tyrosine kinase inhibitors (TKIs) [5, 6], a drug class representing a cornerstone of ccRCC therapy by addressing angiogenesis-related pathways [7].

Functionally, MF is known for inhibiting tumor growth by activating AMP-activated protein kinase (AMPK) and counteracting mechanistic target of rapamycin (mTOR) signaling [8–10]. Additionally, MF can alter microRNA (miR) expression – thereby functioning as an antitumor agent [11, 12]. In specific, MF treatment caused a downregulation of miR-21 in ccRCC cells [13]. In contrast, MF induced miR-205 expression in murine embryonic fibroblasts [14]. This miR is frequently downregulated in cancer, e.g., prostate cancer [15] and ccRCC [16]. Additionally, miR-205 was shown to specifically target *VEGFA* in malignancies such as breast cancer [17] and ccRCC [16]. We therefore investigated whether MF administration influenced miR-205 expression in ccRCC cells – thereby potentially regulating *VEGFA* expression and TKI response in vitro.

Given that a functional loss of the von Hippel-Lindau gene (VHL) is a frequent event in ccRCC pathogenesis and given its role in angiogenesis regulation [18, 19], we finally investigated the influence of the *VHL* status on the miR-205/*VEGFA* axis.

Materials and Methods

Cell Culture and Reagents

Cell lines were obtained from ATCC (American Type Culture Collection, Chicago, IL, USA): HEK293T (ATCC cat# 3216), 786-O (ATCC cat# 1932, VHL^{mut}), and RCC4 (ATCC cat# 11268, VHL^{mut}). Cells were cultured in DMEM high glucose (4.5 g/L), supplemented with 10% fetal calf serum, 2 mmol/L glutamine, and 100 U/mL penicillin/streptomycin (all PAA, Pasching, Austria). HK-2 (ATCC cat# 2190, immortalized human renal proximal tubule epithelial cells) were cultured in keratinocyte serum-free medium supplemented with 0.05 mg/mL bovine pituitary extract, 5 ng/mL human recombinant epidermal growth factor, and 100 U/mL Penicillin/Streptomycin. MF was purchased from Sigma Chemical Co. (St. Louis, MO, USA) and diluted in phosphate-buffered saline. Sunitinib (SUT) and axitinib (AX) were kindly provided by Pfizer (New York, NY, USA) and diluted in DMSO.

Patients and Tissue Sample Preparation

Tumor tissue and adjacent benign tissue of $n = 32$ RCC patients undergoing radical nephrectomy between 2006 and 2010 at the Department of Urology and Pediatric Urology, University Hospital Würzburg, were included in this study. Of note, we did not perform microdissections. Instead, an experienced pathologist macroscopically identified malignant and nonmalignant tissue and confirmed the presence of >90% malignant cell content. Specimens were frozen in liquid nitrogen immediately after resection. Storage was at −80°C until RNA extraction was performed as described below.

Tetracycline-Inducible miR-205 Model in ccRCC Cells

To overexpress miR-205 in ccRCC cells, we used a tetracycline-inducible (Tet-On) model described before [20]. In brief, we cloned the parental miR-205 stem-loop sequence into the lentiviral LT3GEPIR vector (Addgene#11177) using the EcoRI and XhoI restriction sites. Lentivirus was then produced in HEK293T cells using standard protocol, and 786-O and RCC4 cells were subsequently infected with LT3GEPIR lentiviral particles bearing the miR-205 core sequence. Cells were selected using 2 μg/mL puromycin for stable clones 2 weeks prior to experimentation.

Stable Transduction of Wild-Type VHL *in ccRCC Cells*

786-O and RCC4 cells stably expressing VHL^{wt}, and empty vector (EV) controls were a kind gift from Beatrice Griffiths (Institute of Cancer Research, London, UK). In brief, both cell lines were stably transduced using pBabe puro HA-VHL^{wt} (Addgene# 19234) to express HA-tagged VHL^{wt} or pBabe puro (Addgene# 1764) serving as EV controls.

Induction of miR-205 Expression and Drug Treatment

Cells were plated in a final concentration of 1×10^4 to 5×10^4 cells/well in 96-well plates and 1×10^5 to 3×10^5 in 6-well plates. For miR-205 induction, either 1 μg/mL doxycycline (purchased from Sigma-Aldrich, Saint Louis, MS, USA, dissolved in 100% EtOH) or 1 μL/mL 100% EtOH was applied to 786-O and RCC4 cells transduced with LT3GEPIR miR-205. Induction was verified by observation of GFP (green fluorescent protein) expression under a phase-contrast microscope and subsequent real-time quantitative PCR (qRT-PCR). Protein and RNA isolation was carried out 72 h after induction. MF/SUT/AX was added 24 h after plating. Online suppl. Table S1 (for all online suppl. material, see https://doi.org/10.1159/000535025) summarizes compounds and incubation times for each experiment.

Cell Viability Assay

Cells were analyzed with MTS CellTiter96 Proliferation Assay (Promega, Madison, WI, USA) at 490 nm with a monochromator (Bio-Rad, Hercules, FL, USA) according to the manufacturer.

RNA Extraction and Reverse Transcription

Total RNA was extracted from cells after miR-205 induction and/or drug treatment as well as from patient samples using phenol-chloroform extraction (TRIzol agent, Life Technologies, Carlsbad, MN, USA). Total RNA concentration was determined with a bioanalyzer (Agilent, Santa Clara, CA, USA). cDNA was synthesized from total RNA with stem-loop reverse transcription primers according to the TaqMan miR assay protocol for microRNA expression and according to the IMPROM-II reverse transcription kit protocol (Promega, Madison, WI, USA).

Real-Time Quantitative PCR

Mature miR expression was quantified in tissue samples with TaqMan miR assay kits and an Applied Biosystems 7.900HT system. We followed the manufacturer's protocol (Life Technologies, Carlsbad, MN, USA). Expression of snRNA RNU6B served

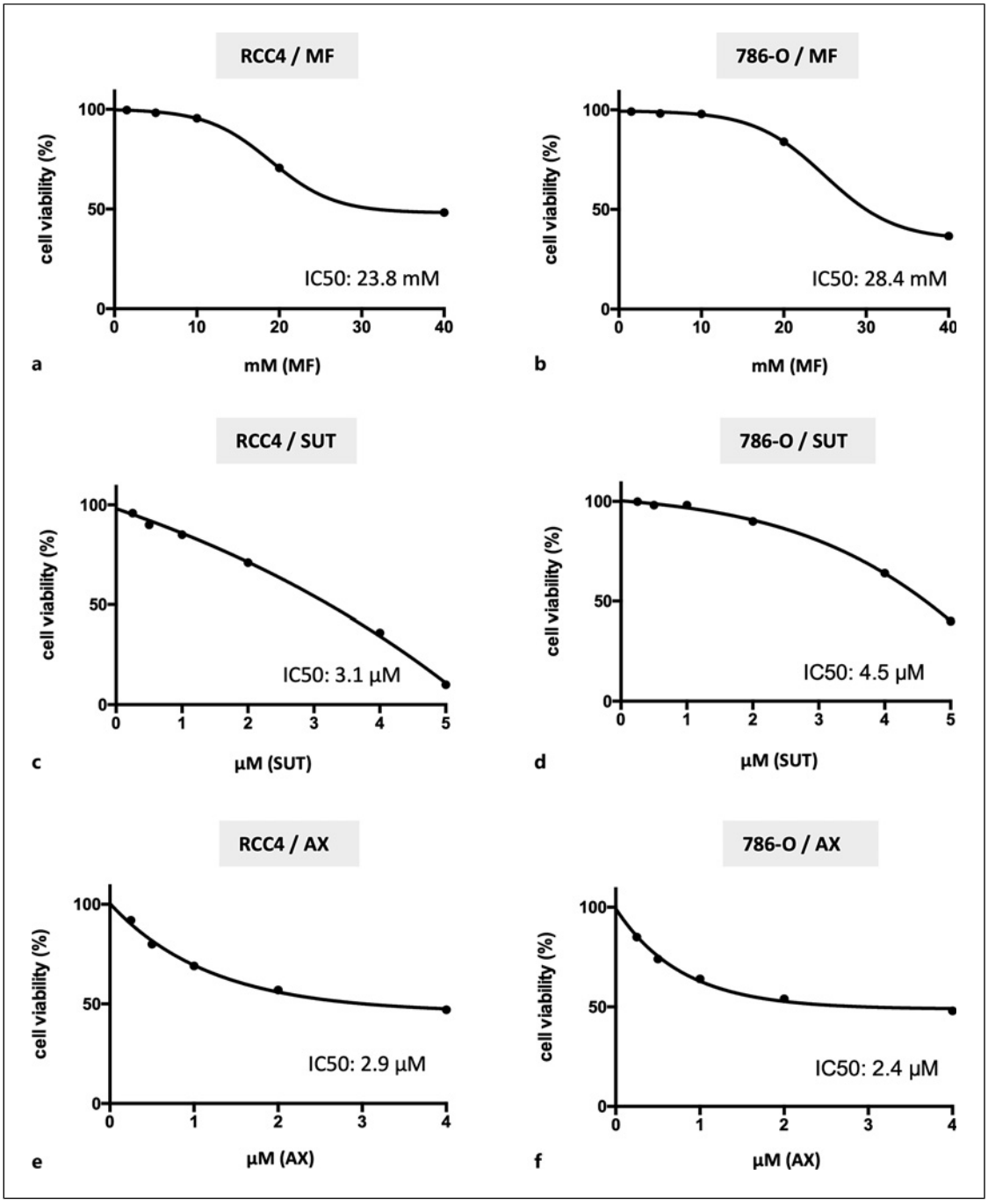

Fig. 1. MTS assays determining relative cell viabilities (in %) for RCC4 and 786-O cells treated with MF (**a**, **b**), SUT (**c**, **d**), and AX (**e**, **f**) for 120 h compared to untreated cells. IC50 values were calculated by using linear regression modeling.

as normalization. Relative miR expression was calculated with the comparative ΔCt method (ΔCt sample = Ct sample - Ct RNU6b). Fold changes in miR expression were determined by the $2^{-\Delta\Delta Ct}$ method. mRNA analysis of *VEGFA* expression was performed according to standard procedures. Expression of β-Actin was used for normalization. All primer sequences are available upon request, if not bought as ready-to-use kits. Mean Ct was determined from triplicate PCRs.

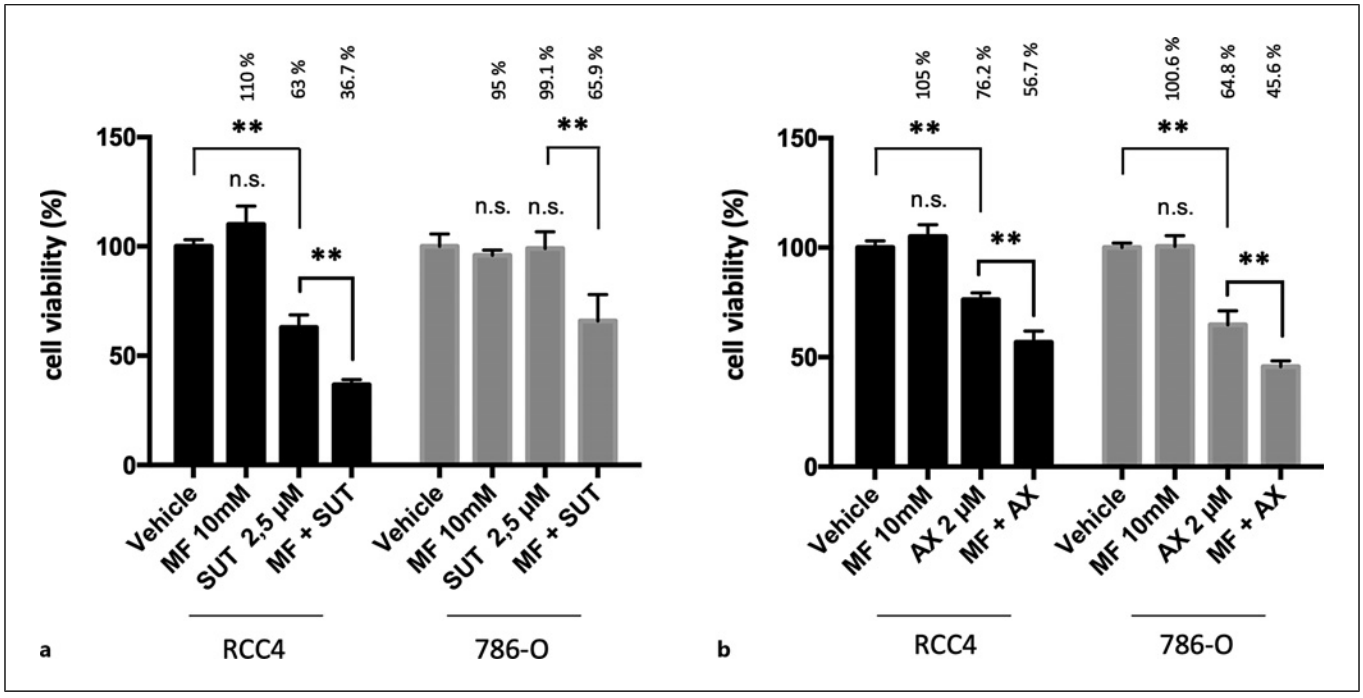

Fig. 2. Synergistic effects for MF and SUT/AX in RCC4 and 786-O cells. MTS assay results (120 h after treatment) for RCC4 and 786-O cells treated with MF, SUT (**a**) or AX (**b**) and a combination of MF and SUT/AX compared to EtOH-treated control cells (vehicle). $^{**}p < 0.01$.

Western Blot Analysis

Cells were lysed in PhosphoSafe (MERCK Life Sciences, Billerica, MA, USA). Equal amounts of protein isolates were separated on SDS-PAGE and transferred to a nitrocellulose membrane (Bio-Rad, Hercules, CA, USA). For *VEGFA* protein expression, we used 1 mg/mL polyclonal antibodies (Abcam, Cambridge, UK). Vimentin (Sigma-Aldrich, Saint Louis, MS, USA) served as loading control. For visualization, we used horseradish peroxidase-coupled secondary antibodies (Abcam and Agilent) and the ECL Plus kit (GE Healthcare, Chalfont St. Giles, UK). iBright FL1000 (Thermo Fisher, Waltham, MS, USA) was used for processing and visualization. All western blots were repeated three times showing comparable results.

Endothelial Sprouting Assay

Assays were performed as described previously [21]. Briefly, human umbilical vein endothelial cells (HUVECs) (PromoCell, C-12205) were cultured overnight in hanging drops in M200 medium with 25% methylcellulose (Sigma, M0512) to form spheroids. Then, spheroids were retrieved and centrifuged at 300 *g* for 5 min. They were embedded into a collagen matrix in a 24-well plate consisting of 43% collagen (3.5 mg/mL, Corning/OMNILAB GmbH & Co. KG # 354236), 41% M200 medium with 25% methylcellulose and 40% fetal calf serum, 15% NaHCO3 (15.6 mg/mL), and 1% 1 M NaOH. Spheroids were incubated for 30 min at 37°C for polymerization of the collagen matrix. Then, medium was added, and cells were incubated for 24 h. Afterward, spheroids were fixed with 4% paraformaldehyde for 20 min at room temperature and washed with PBS. Pictures were taken with a bright-field microscope and analyzed using ImageJ.

Statistical Analysis

Statistical analysis was performed using R 3.10 (http://www.r-project.org), and figures were drawn with GraphPad Prism 7. Pearson's χ^2 test was used to realize intergroup comparison. If two means of continuous data were compared, a two-sided unpaired Student's *t* test was used. miR-205-5p and *VEGFA* mRNA expression data from the TCGA KIRC cohort were accessed via ENCORI (https://starbase.sysu.edu.cn) [22].

Results

Decreased Viabilities of RCC4 and 786-O Cells after MF and TKI Administration

We treated RCC4 and 786-O cells with increasing doses of MF, SUT, or AX. Figure 1 shows relative cell viabilities – IC50 values (defined as 50% relative cell viability) were determined by linear regression and extrapolation. For MF (Fig. 1a, b), MTS assays revealed IC50 values of 23.8 mM for RCC4 and 28.4 mM for 786-O cells. Regarding SUT (Fig. 1c, d), we measured IC50 values of 3.1 µM for RCC4 and 4.5 µM for 786-O cells. IC50 values for AX (Fig. 1e, f) were 2.9 µM (RCC4) and 2.4 µM (786-O), respectively.

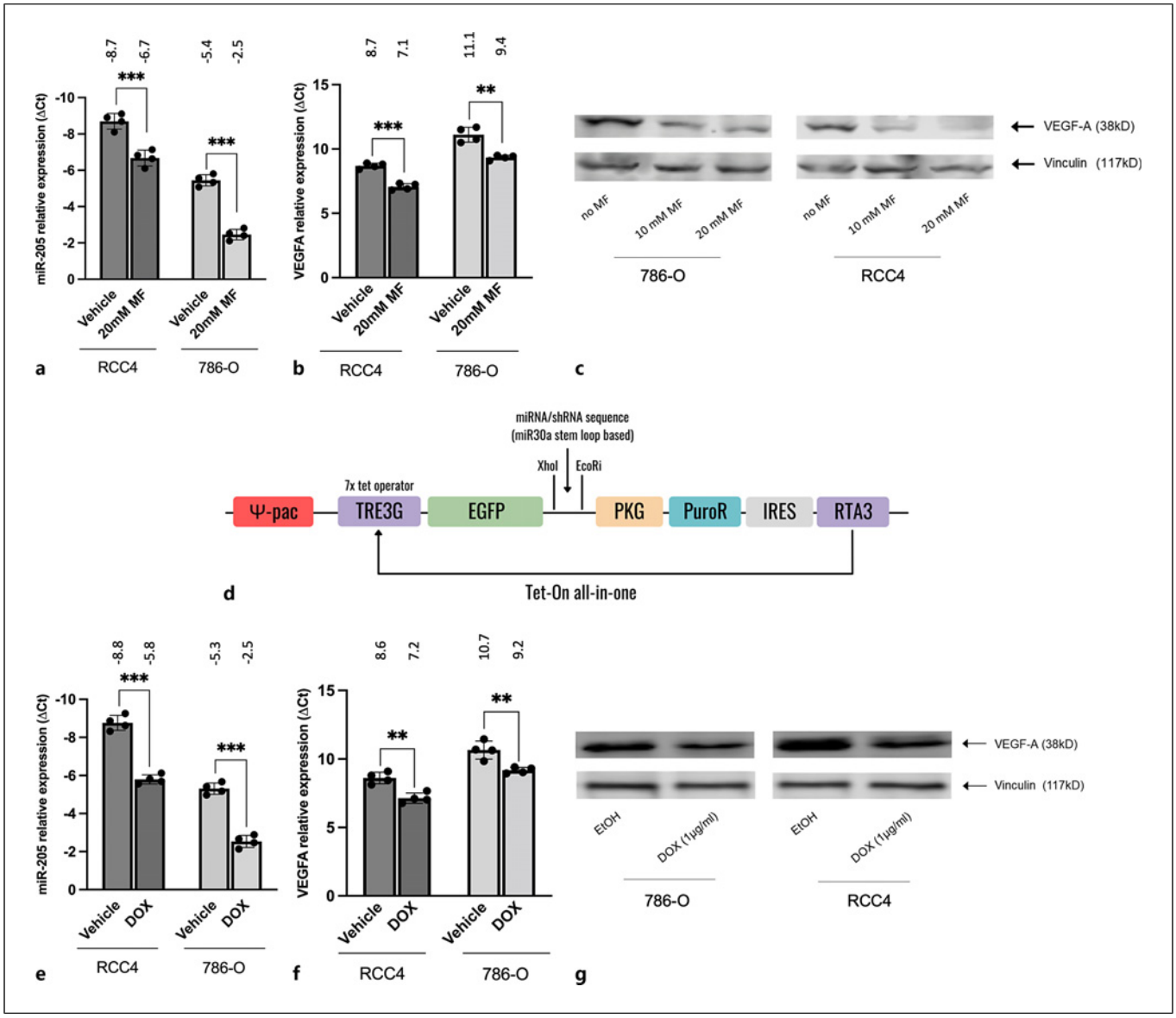

Fig. 3. MF induces miR-205 expression with subsequent downregulation of *VEGFA* in RCC4 and 786-O cells – mimicking the effects on miR-205 and *VEGFA* expression in a doxycycline-inducible model of miR-205 overexpression (Tet-On model). **a**, **b** qRT-PCR confirmed MF-dependent miR-205 upregulation with subsequent *VEGFA* in both cell lines. **c** Western blotting yielded a progressive downregulation of *VEGFA* protein levels with increasing doses of MF (10 mM and 20 mM) in RCC4 and 786-O cells. **d** Tet-On model for miR-205 overexpression. **e**, **f** qRT-PCR experiments determining miR-205 overexpression and *VEGFA* downregulation within the miR-205 Tet-On model for RCC4 and 786-O cells. **g** Diminished *VEGFA* protein expression in miR-205 overexpressing RCC4 and 786-O cells (Tet-On model). **c**, **g** Vinculin was taken as housekeeping protein. $^{**}p < 0.01$, $^{***}p < 0.001$.

Combining MF and TKI Treatment Revealed Synergistic Effects

As illustrated in Figure 2a, single treatment with MF (10 mM) did not significantly alter the viability of RCC4 and 786-O cells, whereas SUT (2.5 μM) significantly diminished the viability of RCC4 cells. In contrast, identical doses of SUT did not significantly change cell viability of 786-O cells. Treating both cell lines with 2 μM AX (Fig. 2b) significantly diminished the viability of RCC4 and 786-O cells. Of note, adding the identical dose of MF (10 mM) to SUT or AX (Fig. 2a, b) augmented TKI effects in RCC4 and 786-O cells – resulting in a significantly lower proportion of viable cells compared to single TKI treatment.

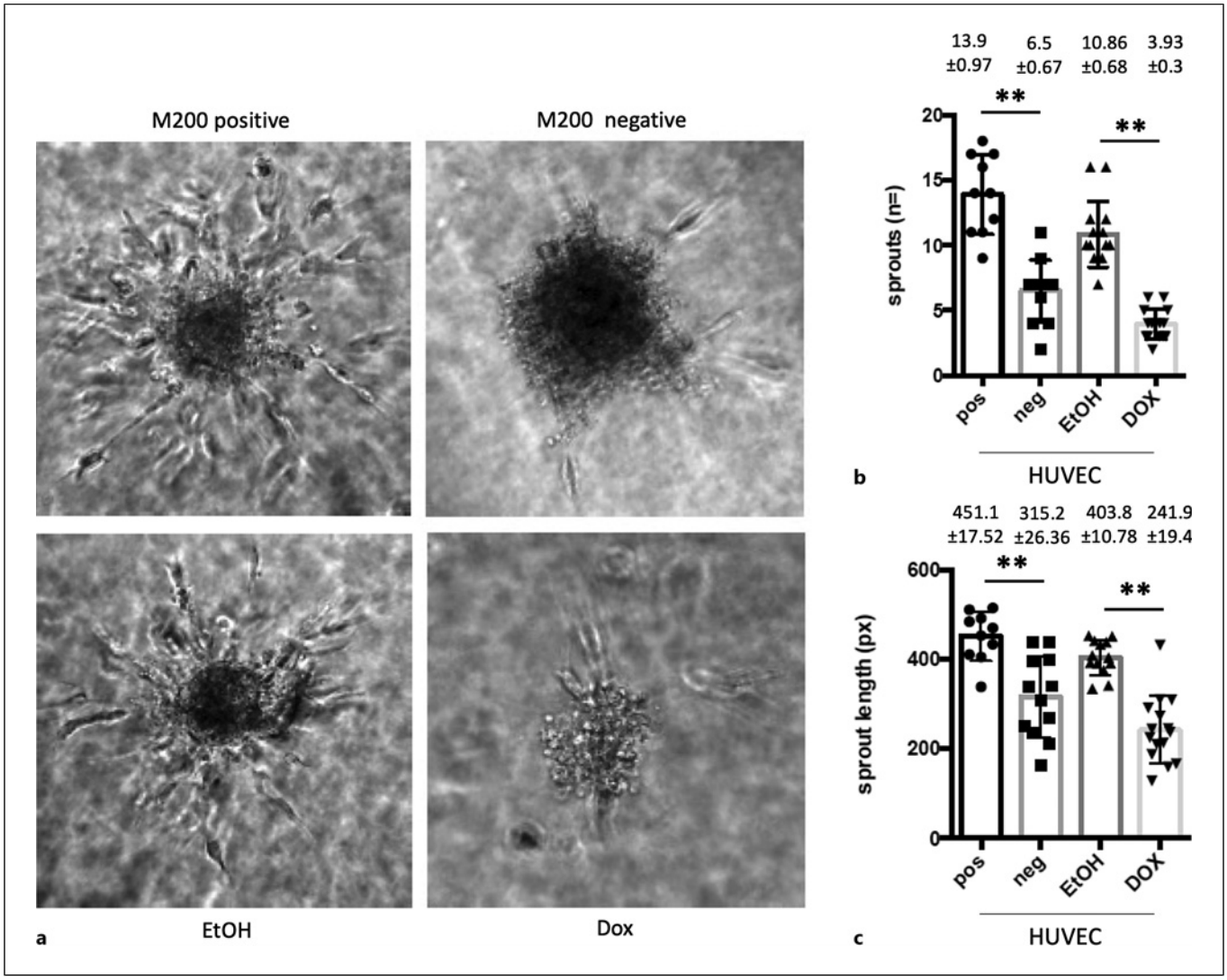

Fig. 4. Number and average length of sprouts from HUVEC cells treated with the supernatant of miR-205-overexpressing ccRCC cells (Tet-On). **a** As illustrated by microscopic images (××40 magnification), doxycycline induction (i.e., miR-205 overexpression) compared to EtOH administration was associated with less (**b**) and shorter vessel sprouts – measured in pixel length by ImageJ (**c**). Presence and absence of recombinant VEGF within M200 medium served as positive and negative control. $^{**}p < 0.01$. Method: cells treated with either EtOH or DOX were cultured overnight in hanging drops → incubated for 24 h → spheroids fixed and washed → pictures taken.

MF Regulated Expression of miR-205 and VEGFA *in ccRCC Cells*

As shown in Figure 3a and b, treating RCC4 and 786-O cells with MF (20 mM) caused a highly significant miR-205 overexpression along with a decreased expression of *VEGFA*. Western blotting confirmed decreased *VEGFA* protein levels after treatment with 20 mM MF for both RCC4 and 786-O cells (Fig. 3c). To examine the role of miR-205 and its regulation of *VEGFA* in ccRCC cells, we used a Tet-On model of miR-205 overexpression (Fig. 3d). For this, qRT-PCR experiments (Fig. 3e, f) affirmed significant overexpression of miR-205 after doxycycline treatment and a significant *VEGFA* downregulation. Western blotting revealed decreased *VEGFA* protein levels in the miR-205 Tet-On model (Fig. 3g). These data suggest that decreased *VEGFA* expression after MF treatment was at least partially caused by MF-driven miR-205 overexpression.

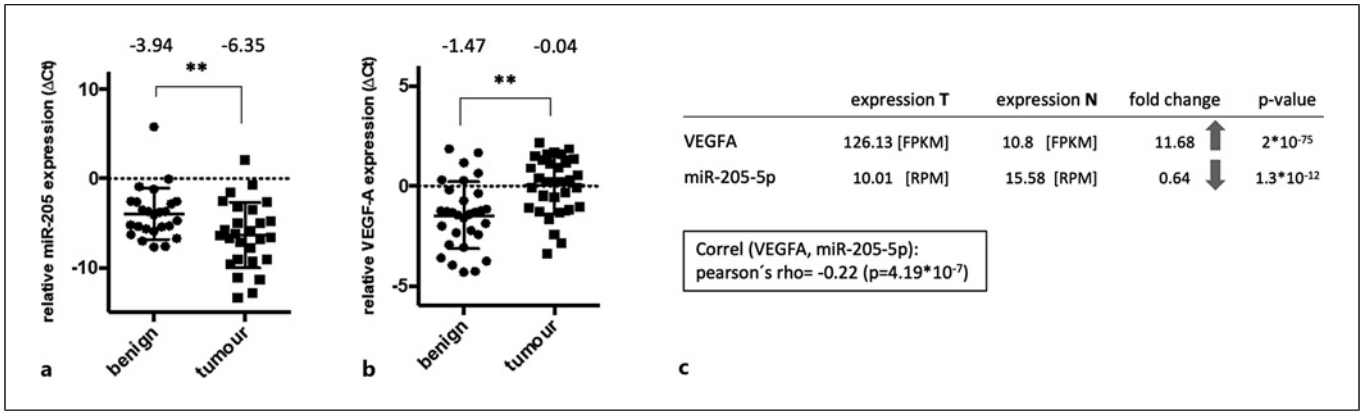

Fig. 5. miR-205 and *VEGFA* expression in RCC. **a** miR-205 is significantly downregulated in malignant tissue of an in-house RCC cohort. **b** *VEGFA* is significantly upregulated in cancerous lesions. **c** Data from the TCGA ccRCC cohort: *VEGFA* is significantly overexpressed in malignant tissue ($n = 523$) compared to benign tissue ($n = 100$). Apart from *VEGFA* upregulation, miR-205 is significantly downregulated in ccRCC specimens – resulting in a significant negative correlation of *VEGFA* and miR-205 expression. FPKM, fragments per kilobase per million mapped reads; RPM, reads per million mapped reads.

Supernatant of miR-205-Overexpressing ccRCC Cells Reduced HUVEC Vessel Sprouting

Treating HUVECs with supernatants of miR-205 overexpressing ccRCC cells dramatically reduced their sprouting ability (Fig. 4a) – in terms of less endothelial sprouts (Fig. 4b) and shorter sprouts (Fig. 4c). These results indicate that high levels of miR-205 in ccRCC cells severely impede angiogenesis initiation in endothelial cells.

miR-205 and VEGFA *Expression in RCC Tissue*

Next, we analyzed the expression of miR-205 and *VEGFA* in an in-house RCC cohort ($n = 32$) with corresponding malignant and adjacent benign tissue. qRT-PCR analyses revealed significantly lower expression levels of miR-205 (median ΔCt −3.94 in benign tissue vs. ΔCt −6.35 in tumors, $p < 0.01$, Fig. 5a) and significantly higher levels of *VEGFA* in cancer tissue (median ΔCt −1.47 in benign tissue vs. ΔCt −0.04 in tumors, $p < 0.01$, Fig. 5b). In line with the in-house cohort, the TCGA database (Fig. 5c) also revealed a downregulation of miR-205 accompanied by a *VEGFA* upregulation (Pearson's $\rho = -0.22$, $p < 0.01$).

VHL *Influences miR-205 and* VEGFA *Expression as well as Drug Sensitivity of ccRCC Cells*

To determine a potential influence of *VHL* on miR-205 and *VEGFA* expression, we used a constitutive model for VHL^{wt} overexpressing clones of originally VHL^{mut} RCC4 and 786-O cells. qRT-PCR analyses compared EV and VHL^{wt} RCC4 and 786-O cells in terms of miR-205 (Fig. 6a) and *VEGFA* expression (Fig. 6b), thereby confirming a significant upregulation of miR-205 in VHL^{wt} RCC4 and 786-O cells. Correspondingly, *VEGFA* was significantly lower in VHL^{wt}-expressing ccRCC cell lines. Immortalized, nonmalignant HK-2 cells served as negative control and displayed significantly higher miR-205 as well as lower *VEGFA* expression compared to ccRCC cells. Western blotting (Fig. 6c) showed markedly decreased protein amounts of *VEGFA* in VHL^{wt}-expressing RCC4 and 786-O cells. In the following, cell viability assays revealed a significantly higher sensitivity of VHL^{wt} RCC4 and 786-O cells toward MF and SUT (Fig. 6d) compared to VHL^{mut} parental RCC4 and 786-O cells.

Discussion

Growing evidence suggests tumor-suppressive effects of MF in various malignancies [1]. From a clinical perspective, regular MF intake was associated with prolonged overall survival in ccRCC patients treated with SUT [5, 6]. Functionally, findings from MF-treated murine embryonic fibroblasts [14] suggested that MF can upregulate cellular miR-205 expression. Therefore, we investigated whether MF also modulated miR-205 expression in ccRCC cells. Given the miR-205-mediated regulation of *VEGFA* in entities such as breast cancer, ovarian cancer, glioblastoma multiforme, and ccRCC itself [16, 23–25], we examined whether MF-caused regulation of miR-205 expression was sufficient to modulate *VEGFA* expression in ccRCC cells.

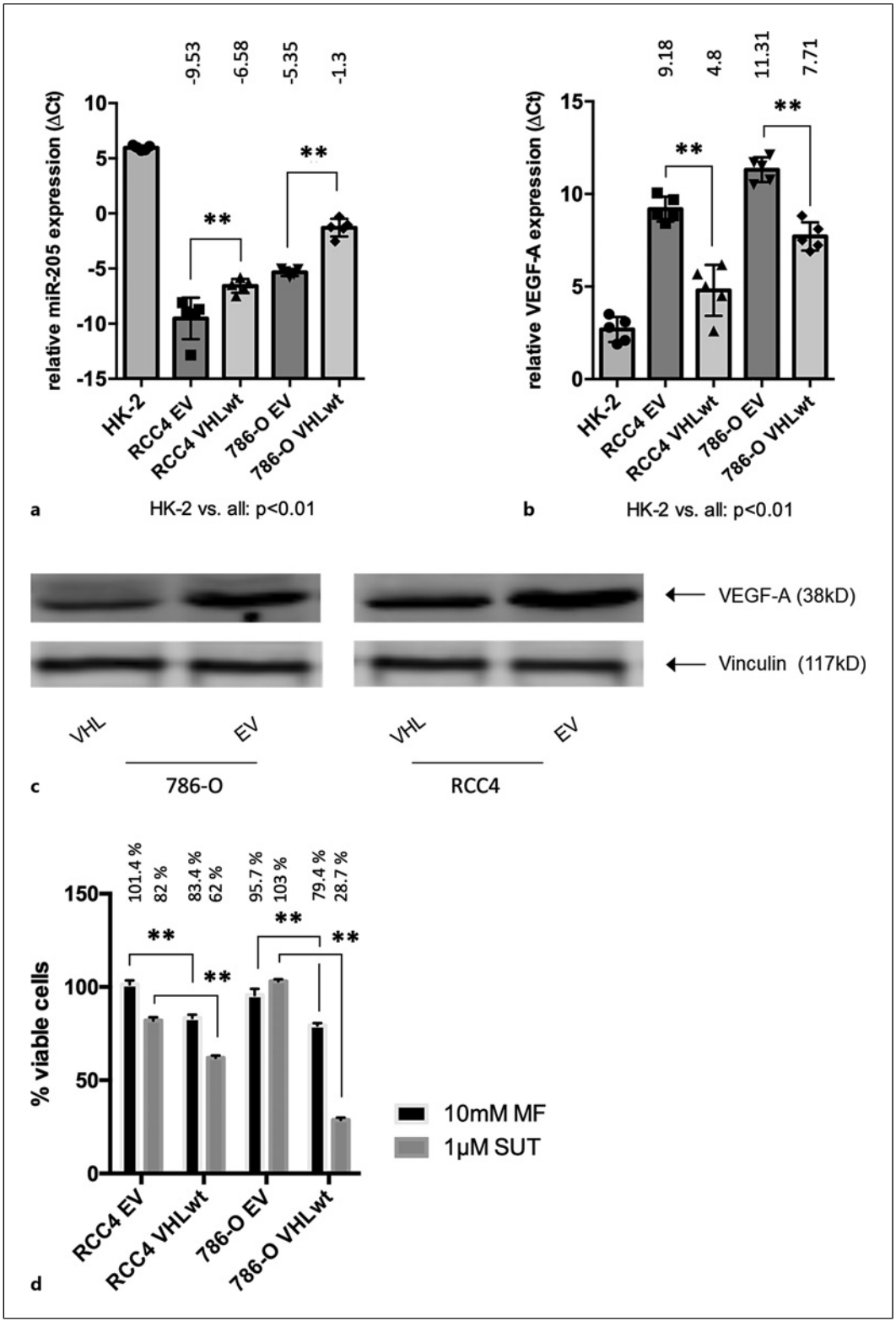

Fig. 6. Expression of miR-205 and *VEGFA* in RCC4 and 786-O cells depending on *VHL* status. **a**, **b** *VHLwt* RCC4 and 786-O cells exhibited higher levels of miR-205 and correspondingly lower levels of *VEGFA*. HK-2 cells were taken as control. **c** *VHLwt* RCC4 and 786-O cells were characterized by decreased VEGF protein levels. Vinculin served as a housekeeping protein. **d** *VHLwt* RCC cells were significantly more sensitive toward MF and SUT treatment. $^{**}p < 0.01$.

MF Induced miR-205 Expression with Subsequent Targeting of VEGFA *in ccRCC Cells*

The IC50 values for MF were markedly higher for RCC4 and 786-O cells compared to IC50 counts reported previously for colon carcinoma [26] and prostate cancer cell lines [27]. Still, these values were substantially lower than those previously found for MF treatment in nonmalignant HK-2 cells [28]. Regarding SUT treatment of HK-2 cells, researchers also reported higher IC50 counts [29, 30] compared to SUT treatment of RCC4 and 786-O cells shown here (see online suppl. Table S2).

Regarding dual treatment of RCC4 and 786-O cells, we observed a significant synergistic effect for the combination of MF and TKI treatment with SUT or AX for both cell lines. Additionally, MF administration significantly induced the expression of miR-205 in both ccRCC cell lines. Apart from this specific trait, our Tet-On model confirmed that elevated miR-205 expression regulated the expression of *VEGFA* in RCC4 and 786-O cells. In addition, analyses of ccRCC specimens of an in-house RCC cohort and the TCGA database (KIRC cohort) revealed a downregulation of miR-205 in ccRCC tissue along with an upregulation of *VEGFA*.

In previous literature, MF was reported to act in both directions – either as antiangiogenic [31, 32] or as proangiogenic compound by, among other things, upregulating *VEGFA* [33, 34]. However, MF-mediated induction of miR-205 with subsequent decrease in *VEGFA* expression clearly represents a novel tumor suppressive and antiangiogenic trait of MF in ccRCC cells.

Impact of miR-205 Overexpressing ccRCC Cells on Angiogenesis Initiation in HUVEC Cells

We now wanted to take a closer look at the potential impact of MF on angiogenesis/vessel sprouting in vitro. For this reason, we performed HUVEC sprouting assays to determine an influence of the MF/miR-205/*VEGFA* axis. The analysis of HUVEC clusters treated with the medium supernatant of miR-205-overexpressing ccRCC cells revealed significantly less vessel sprouts. Moreover, sprouts from HUVEC cells treated with the supernatant from doxycycline-induced cells were significantly shorter. As miR-205 can regulate the expression of a variety of target genes, this experiment could not show an exclusive effect of the miR-205/*VEGFA* axis. However, targeting of *VEGFA* could at least partly explain the antiangiogenic effect of miR-205 observed. Taken together, the results at the very least strengthen the angiogenesis-inhibiting role of MF and miR-205 in ccRCC cells.

VHL *Status Modulated the miR-205/*VEGFA *Axis in ccRCC Cells*

In general, loss of *VHL* function activates hypoxia-inducible factor (HIF) signaling, leading to an increased expression of angiogenic growth factors [18, 19]. Given the crucial role of neo-angiogenesis in ccRCC, it is not astonishing that *VHL* gene defects appear in ~75% of sporadic ccRCC [35]. For this reason, we were interested in whether the MF/miR-205/*VEGFA* axis was controlled by the *VHL* status of the ccRCC cells and compared the originally VHL^{mut} RCC4 and 786-O cell lines with VHL^{wt} RCC4 and 786-O cells. Of note, *VHL* status significantly determined miR-205 and *VEGFA* expression in RCC4 and 786-O cells. Our results suggest that miR-205 should be regarded as a *VHL*-regulated miR, a trait previously known for candidates such as miR-210 and miR-182-5p [36]. Moreover, the intersection of MF- and *VHL*-dependent angiogenic signaling strengthens the protective and antiangiogenic role of MF in ccRCC cells.

To strengthen the rationale for adding MF to antiangiogenic therapies in patients with ccRCC, additional experiments could be performed. Further analyzing the effect of MF on *VHL*-mediated, *HIF*-related signaling and its downstream targets could provide valuable insights regarding TKI interactions. Given that MF was already shown to regulate *HIF1*α [37], this research could pave the way for a similar interaction of MF with HIF2α inhibitors like belzutifan, which are currently tested in clinical trials [38, 39]. Of note, miR-205 expression itself appears to be regulated by *HIF*-mediated signaling [40]. This trait highlights the need for a better understanding of miR networks, as other miRs like miR-126, which also serves as a biomarker candidate in ccRCC [41], were shown to regulate *HIF1a* in turn [42]. Apart from counteracting angiogenic signaling, other MF effects such as inhibition of mitochondrial function could also contribute to the clinically observed added value of MF in TKI trials – as recent findings suggest that mitochondrial signaling could also play a crucial role in ccRCC [43].

Conclusions

Our results shed light on novel aspects of MF as a tumor suppressor in ccRCC cells. MF-mediated induction of miR-205 with subsequent downregulation of its target gene *VEGFA* could be one explanatory approach for the clinical synergism of MF and TKI in cancer patients. Of note, the MF/miR-205/*VEGFA* axis was critically influenced by the *VHL* status of the cancer cells. Clinically, our data provide a further rationale for examining MF in ccRCC trials.

Statement of Ethics

The study was approved by the Ethical Review Board of the Julius Maximilians University Würzburg, Germany (No. 136/08), and written informed consent was obtained from all patients participating.

Conflict of Interest Statement

The authors have no conflicts of interest to declare.

Funding Sources

M.K. was funded by a personal grant from Else-Kröner-Foundation (Else Kröner Integrative Clinician Scientist College for Translational Immunology, University Hospital Würzburg, Germany). Pfizer (New York, NY, USA) kindly provided sunitinib and axitinib.

Author Contributions

Conceptualization: M.K., J.F., B.K., A.S., and C.K.; methodology: M.K., B.K., A.S., and C.K.; software and visualization: F.R., A.M., and C.K.; validation: H.K., B.K., and A.S.; formal analysis: M.K., A.M., S.J.R., and C.K.; investigation: M.J.K., J.F., F.R., S.J.R., A.M., and C.K.; resources: F.R., S.J.R., and C.K.; data curation: C.K.; writing: M.K., M.J.K., and C.K.; writing – review and editing: M.K., A.M., M.J.K., and C.K.; supervision: H.K., A.S., and C.K.; project administration: C.K.; and funding acquisition: H.K., B.K., A.S., and C.K.

Data Availability Statement

All data generated or analyzed during this study are included in this article. Further inquiries can be directed to the corresponding author. The results shown here are in part based upon data generated by the TCGA Research Network: https://www.cancer.gov/tcga.

References

1 Schulten HJ. Pleiotropic effects of Metformin on cancer. Int J Mol Sci. 2018;19(10):2850.
2 Luo X, Chen X, Wang L, Yang B, Cai S. Metformin adjunct with antineoplastic agents for the treatment of lung cancer: a meta-analysis of randomized controlled trials and observational cohort studies. Front Pharmacol. 2021;12:639016.
3 Coyle C, Cafferty FH, Vale C, Langley RE. Metformin as an adjuvant treatment for cancer: a systematic review and meta-analysis. Ann Oncol. 2016;27(12):2184–95.
4 Tseng CH. Use of Metformin and risk of kidney cancer in patients with type 2 diabetes. Eur J Cancer. 2016;52:19–25.
5 Hamieh L, McKay RR, Lin X, Moreira RB, Simantov R, Choueiri TK. Effect of Metformin use on survival outcomes in patients with metastatic renal cell carcinoma. Clin Genitourin Cancer. 2017;15(2):221–9.
6 Keizman D, Ish-Shalom M, Sella A, Gottfried M, Maimon N, Peer A, et al. Metformin use and outcome of Sunitinib treatment in patients with diabetes and metastatic renal cell carcinoma. Clin Genitourin Cancer. 2016;14(5):420–5.
7 Argentiero A, Solimando AG, Krebs M, Leone P, Susca N, Brunetti O, et al. Anti-angiogenesis and immunotherapy: novel paradigms to envision tailored approaches in renal cell-carcinoma. JCM. 2020;9(5):1594.
8 Shaw RJ, Lamia KA, Vasquez D, Koo SH, Bardeesy N, DePinho RA, et al. The kinase LKB1 mediates glucose homeostasis in liver and therapeutic effects of Metformin. Science. 2005;310(5754):1642–6.
9 Ben Sahra I, Le Marchand-Brustel Y, Tanti JF, Bost F. Metformin in cancer therapy: a new perspective for an old antidiabetic drug? Mol Cancer Ther. 2010;9(5):1092–9.
10 Ben Sahra I, Regazzetti C, Robert G, Laurent K, Le Marchand-Brustel Y, Auberger P, et al. Metformin, independent of AMPK, induces MTOR inhibition and cell-cycle arrest through REDD1. Cancer Res. 2011;71(13):4366–72.
11 Zhou JY, Xu B, Li L. A new role for an old drug: Metformin targets MicroRNAs in treating diabetes and cancer. Drug Dev Res. 2015;76(6):263–9.
12 Jiang X, Ma N, Wang D, Li F, He R, Li D, et al. Metformin inhibits tumor growth by regulating multiple MiRNAs in human cholangiocarcinoma. Oncotarget. 2015;6(5):3178–94.
13 Kalogirou C, Schäfer D, Krebs M, Kurz F, Schneider A, Riedmiller H, et al. Metformin-derived growth inhibition in renal cell carcinoma depends on MiR-21-mediated PTEN expression. Urol Int. 2016;96(1):106–15.
14 Cufí S, Vazquez-Martin A, Oliveras-Ferraros C, Quirantes R, Segura-Carretero A, Micol V, et al. Metformin lowers the threshold for stress-induced senescence: a role for the MicroRNA-200 family and MiR-205. Cell Cycle. 2012;11(6):1235–46.
15 Kalogirou C, Spahn M, Krebs M, Joniau S, Lerut E, Burger M, et al. MiR-205 is progressively down-regulated in lymph node metastasis but fails as a prognostic biomarker in high-risk prostate cancer. IJMS. 2013;14(11):21414–34.
16 Huang J, Wang X, Wen G, Ren Y. MiRNA-205-5p functions as a tumor suppressor by negatively regulating VEGFA and PI3K/akt/MTOR signaling in renal carcinoma cells. Oncol Rep. 2019;42(5):1677–88.
17 Hu Y, Qiu Y, Yagüe E, Ji W, Liu J, Zhang J. MiRNA-205 targets VEGFA and FGF2 and regulates resistance to chemotherapeutics in breast cancer. Cell Death Dis. 2016;7(6):e2291.
18 Shenoy N, Pagliaro L. Sequential pathogenesis of metastatic VHL mutant clear cell renal cell carcinoma: putting it together with a translational perspective. Ann Oncol. 2016;27(9):1685–95.
19 Gudas LJ, Fu L, Minton DR, Mongan NP, Nanus DM. The role of HIF1α in renal cell carcinoma tumorigenesis. J Mol Med Berl. 2014;92(8):825–36.
20 Kalogirou C, Linxweiler J, Schmucker P, Snaebjornsson MT, Schmitz W, Wach S, et al. MiR-205-Driven downregulation of cholesterol biosynthesis through SQLE-inhibition identifies therapeutic vulnerability in aggressive prostate cancer. Nat Commun. 2021;12(1):5066.
21 Eelen G, Dubois C, Cantelmo AR, Goveia J, Brüning U, DeRan M, et al. Role of glutamine synthetase in angiogenesis beyond glutamine synthesis. Nature. 2018;561(7721):63–9.
22 Li JH, Liu S, Zhou H, Qu LH, Yang JH. StarBase v2.0: decoding MiRNA-CeRNA, MiRNA-NcRNA and protein–RNA interaction networks from large-scale CLIP-seq data. Nucl Acids Res. 2014;42(Database issue):D92–7.
23 Wu H, Zhu S, Mo YY. Suppression of cell growth and invasion by MiR-205 in breast cancer. Cell Res. 2009;19(4):439–48.
24 Yue X, Wang P, Xu J, Zhu Y, Sun G, Pang Q, et al. MicroRNA-205 functions as a tumor suppressor in human glioblastoma cells by targeting VEGF-A. Oncol Rep. 2012;27(4):1200–6.
25 Li J, Li L, Li Z, Gong G, Chen P, Liu H, et al. The role of MiR-205 in the VEGF-mediated promotion of human ovarian cancer cell invasion. Gynecol Oncol. 2015;137(1):125–33.

26 Zakikhani M, Dowling RJO, Sonenberg N, Pollak MN. The effects of adiponectin and Metformin on prostate and colon neoplasia involve activation of AMP-activated protein kinase. Cancer Prev Res. 2008;1(5):369–75.
27 Fendt SM, Bell EL, Keibler MA, Davidson SM, Wirth GJ, Fiske B, et al. Metformin decreases glucose oxidation and increases the dependency of prostate cancer cells on reductive glutamine metabolism. Cancer Res. 2013;73(14):4429–38.
28 Yang X, Ding H, Qin Z, Zhang C, Qi S, Zhang H, et al. Metformin prevents renal stone formation through an antioxidant mechanism in vitro and in vivo. Oxid Med Cell Longev. 2016;2016:4156075.
29 Xiao J, Wang J, Yuan L, Hao L, Wang D. Study on the mechanism and intervention strategy of Sunitinib induced nephrotoxicity. Eur J Pharmacol. 2019;864:172709.
30 Amaro F, Pisoeiro C, Valente MJ, Bastos ML, Guedes de Pinho P, Carvalho M, et al. Sunitinib versus pazopanib dilemma in renal cell carcinoma: new insights into the in vitro metabolic impact, efficacy, and safety. Int J Mol Sci. 2022;23(17):9898.
31 Orecchioni S, Reggiani F, Talarico G, Mancuso P, Calleri A, Gregato G, et al. The biguanides Metformin and phenformin inhibit angiogenesis, local and metastatic growth of breast cancer by targeting both neoplastic and microenvironment cells. Int J Cancer. 2015;136(6):E534–44.
32 Ying Y, Ueta T, Jiang S, Lin H, Wang Y, Vavvas D, et al. Metformin inhibits ALK1-mediated angiogenesis via activation of AMPK. Oncotarget. 2017;8(20):32794–806.
33 Phoenix KN, Vumbaca F, Claffey KP. Therapeutic Metformin/AMPK activation promotes the angiogenic phenotype in the ERalpha negative MDA-MB-435 breast cancer model. Breast Cancer Res Treat. 2009;113(1):101–11.
34 Martin MJ, Hayward R, Viros A, Marais R. Metformin accelerates the growth of BRAF V600E-driven melanoma by upregulating VEGF-A. Cancer Discov. 2012;2(4):344–55.
35 Maher ER. Genomics and epigenomics of renal cell carcinoma. Semin Cancer Biol. 2013;23(1):10–7.
36 Schanza LM, Seles M, Stotz M, Fosselteder J, Hutterer GC, Pichler M, et al. MicroRNAs associated with von hippel-lindau pathway in renal cell carcinoma: a comprehensive review. Int J Mol Sci. 2017;18(11):2495.
37 Hart PC, Kenny HA, Grassl N, Watters KM, Litchfield LM, Coscia F, et al. Mesothelial cell HIF1α expression is metabolically downregulated by Metformin to prevent oncogenic tumor-stromal crosstalk. Cell Rep. 2019;29(12):4086–98.e6.
38 Choueiri TK, Kaelin WG. Targeting the HIF2–VEGF Axis in renal cell carcinoma. Nat Med. 2020;26(10):1519–30.
39 Jonasch E, Donskov F, Iliopoulos O, Rathmell WK, Narayan VK, Maughan BL, et al. Belzutifan for renal cell carcinoma in von Hippel–lindau disease. N Engl J Med. 2021;385(22):2036–46.
40 Gandellini P, Giannoni E, Casamichele A, Taddei ML, Callari M, Piovan C, et al. MiR-205 hinders the malignant interplay between prostate cancer cells and associated fibroblasts. Antioxid Redox Signal. 2014;20(7):1045–59.
41 Kotlyar MJ, Krebs M, Solimando AG, Marquardt A, Burger M, Kübler H, et al. Critical evaluation of a MicroRNA-based risk classifier predicting cancer-specific survival in renal cell carcinoma with tumor thrombus of the inferior vena cava. Cancers. 2023;15(7):1981.
42 Single-cell transcriptome analysis reveals embryonic endothelial heterogeneity at spatiotemporal level and multifunctions of MicroRNA-126 in mice|arteriosclerosis, thrombosis, and vascular biology. Available from: https://www.ahajournals.org/doi/10.1161/ATVBAHA.121.317093 (accessed on 17 August 2023).
43 Marquardt A, Solimando AG, Kerscher A, Bittrich M, Kalogirou C, Kübler H, et al. Subgroup-independent mapping of renal cell carcinoma—machine learning reveals prognostic mitochondrial gene signature beyond histopathologic boundaries. Front Oncol. 2021;11:621278.